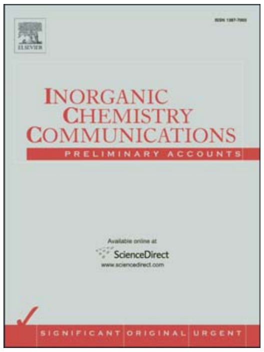

Layered crystalline chiral salen Mn(III) complexes immobilized on organic polymer–inorganic hybrid zinc phosphonate-phosphate as efficient and reusable catalysts for the unfunctionalized olefin epoxidation

Jing Huang, Li Yuan, Jiali Cai, Xiaohong Chen, Dengwei Qi

PII: S1387-7003(16)30001-6
DOI: doi: 10.1016/j.inoche.2016.01.001
Reference: INOCHE 6205

To appear in: *Inorganic Chemistry Communications*

Received date: 25 October 2015
Revised date: 1 January 2016
Accepted date: 3 January 2016

Please cite this article as: Jing Huang, Li Yuan, Jiali Cai, Xiaohong Chen, Dengwei Qi, Layered crystalline chiral salen Mn(III) complexes immobilized on organic polymer–inorganic hybrid zinc phosphonate-phosphate as efficient and reusable catalysts for the unfunctionalized olefin epoxidation, *Inorganic Chemistry Communications* (2016), doi: 10.1016/j.inoche.2016.01.001

Layered crystalline chiral salen Mn(III) complexes immobilized on organic polymer–inorganic hybrid zinc phosphonate-phosphate as efficient and reusable catalysts for the unfunctionalized olefin epoxidation

Jing Huang,[*a,b] LiYuan,[a] Jiali Cai,[c] Xiaohong Chen,[a] Dengwei Qi[d]

[a] Research Center for Advanced Computation, Xihua University; College of Science, Xihua University, Chengdu, 610039, PR China. E-mail:hj41012@163.com;
[b] Institute for Clean Energy & Advanced Materials, Southwest University, Chongqing 400715, PR China.
[c] College of Rongchang, Southwest University, Chongqing, PR China.
[d] Ba Shu Middle School, Chongqing 400023, PR China.

Abstract

Chiral Mn(III) salen complexes grafted on ZnPS-PVPA (zinc poly(styrene-phenylvinylphosphonate)-phosphate) upon alkyldiamines through a facile method are evaluated by the asymmetric epoxidation of unfunctionalized olefins. Superior catalytic performances are obtained (conv%, up to >99; ee%, up to >99) whenever with *m*-CPBA or NaClO or $NaIO_4$ as the oxidant. The additives such as NMO, PPNO as well as imidazole play different roles in the corresponding oxidation system. In addition, the supported catalysts could be reused nine times with the retention of their efficiency. These results highlight the potentiality of ZnPS-PVPA as the support for immobilizing chiral salen Mn (III) to be employed in oxidation reactions.

Keywords: Asymmetric epoxidation; unfunctionalized olefins; Jacobsen’s catalyst; heterogeneous catalyst; alkyldiamines

Introduction

Asymmetric epoxidation of unfunctionalized prochiral olefins, catalyzed by chiral (salen) Mn (III) complexes, has proven to be one of the most useful reactions in organic syntheses since the obtained chiral epoxides contain two new stereocentres and can be easily transformed into a large variety of compounds active in the industrial, biological, pharmaceutical and agricultural fields [1-8]. Although great success has been achieved, the recovery and reuse of such Jacobsen's chiral salen Mn(III) complex is often troublesome [9-12]. Therefore, efforts have been put on heterogenizing the Jacobsen catalyst by anchoring chiral (salen)Mn(III) complexes on solid surfaces in order to enhance their stability, activity, selectivity, recovery and recycling [13-18].

We have devoted ourselves to immobilizing homogeneous chiral salen Mn(III) on a series of hybrid materials, such as zirconium oligostyrenylphosphonate-phosphate (ZSPP) and zirconium poly (styrene-phenylvinylphosphonate)-phosphate (ZPS-PVPA) and zinc poly(styrene-phenylvinyl phosphonate)-phosphate (ZnPS-PVPA) as well as calcium poly(styrene-phenylvinyl-phosphonate)-phosphate (CaPS-PVPA). Moreover, the heterogeneous chiral salen Mn(III) catalysts indicate superior disposition in asymmetric epoxidation of unfunctionalized olefins[19-26].

With the purpose of having clearer insight into surface anchoring that assures no catalyst leaching and high efficiency, we have now developed salen Mn(III) complex immobilized on ZnPS-PVPA through alkyldiamines, especially designed to maintain the Mn(III) environment unaltered after surface grafting. The aim of this work is to evaluate the influence of the synergy of ZnPS-PVPA and the linkers as well as the chiral ligand on the performance and stability of the heterogeneous catalysts.

Scheme 1

---

*Corresponding author: Fax: +86 288772 0200; Tel: +86 288772 0037; E-mail: hj41012@163.com;

Scheme 2

All the supported catalysts **4a-d** and chiral salen Mn(III)Cl have indicated the same band at 1638 cm^{-1} (Fig. S1) owing to the vibration of imine group. According to the azomethene (C=N) stretching band, chiral salen Mn(III)Cl appear at 1613 cm^{-1} and the supported catalysts emerge at the vicinity of 1617 cm^{-1}. The band around 3408 cm^{-1} is observed for the catalysts, which is ascribed to the stretching vibration of N-H groups. The stretching vibration at 1030 cm^{-1} which is assigned to characteristic vibrations of the phosphonate and phosphate in the support, is obviously weakened by virtue of the electronic structure changes for the host-guest interaction.

The spectra of **4a-d** have displayed features similar to those of chiral salen Mn(III)Cl on the basis of UV-vis observation (Fig. S2). The band at 335 nm could be attributed to the charge transfer transition of salen ligand. The band at 433 nm is due to the ligand-to-metal charge transfer transition. The bands at 510 nm is assigned to the d-d transition of salen Mn(III) complex. There manifest some deviations owing to an interaction between the salen Mn(III) complex and the alkyldiamine modified ZnPS-PVPA.

According to the catalyst **4d** (shown in Fig. 1), the initial weight loss is 3.5% below 180℃, which is due to surface-bound or intercalated water in this stage. In the temperature range of 180-700℃, the organic moieties decompose, accompanied with 56.8% weight loss in this stage. Obviously, the catalyst **4d** still keep high stability lower than 180℃. In general, organic reactions of heterogeneous catalysis are carried out below 180℃. Therefore, the catalyst **4d** has adequate thermal stabilities to be applied in heterogeneous catalytic reactions.

Fig. 1

Based on the desorption isotherm (Fig. 2), BJH analysis indicates a broad and non-uniform distribution of pore size (in the range 2-18 nm), which demonstrates that the mesoporous structure exist in the catalyst. The nitrogen adsorption-desorption isotherms are characteristic type V, accompanied with a sharp increase in N_2 adsorption at higher P/P_0 values (~0.9) and a distinct hysteresis loop (type H_1). The pore diameters of the particles are mainly varied from 1nm to 18 nm, and a small quantity of the particles are below 2 nm as well as the less is distributed over 50 nm in diameter.

Fig. 2

The corresponding textural parameters calculated by N_2 adsorption-desorption isotherms and Mn content of the immobilized catalysts are shown in Table 1.

Table 1

By means of chloromethylation, obvious increases are observed in BET surface area (**1** vs **2**, from 4.9 to 36.9 m^2/g), and in the pore volume (**1** vs **2**, from 1.3 to 18.82×10^{-2} cm^3/g) as well as in the average pore diameter (**1** vs **2**, from 3.5 to 10.21 nm). Although the chloromethylation of the support contributes to the interlayer distance enlarged, the chloromethyl is relatively small so that the corresponding textural parameters still increase. In contrast with this phenomenon, decreases are observed in BET surface area (**2** vs **4d**, from 36.9 to 28.02 m^2/g) and in the pore volume (**2** vs **4d**, from 18.82 to 4.442×10^{-2} cm^3/g) as well as in the average pore diameter (**2** vs 4d, from 10.21 to 0.61 nm) upon the immobilization of salen Mn (III) on ZnPS-PVPA. Owing to the steric bulkyl salen Mn (III) introduced in ZnPS-PVPA, some caves, holes and channels would be occupied, which contribute to the corresponding structure parameters ultimately decreasing. On account of these facts, it could be deduced that some chiral salen Mn (III) complexes are immobilized on the external surface of ZnPS-PVPA and others are inserted into the mesopores.

Fig. 3

According to SEM of **4d** (Fig. 3B)**,** the surface morphology varies from the smooth anomalous structure for ZnPS-PVPA (Fig. 3A) to the loose amorphous configuration after the immobilization of salen Mn (III). And many small caves and channels with irregular shapes also exist, which would increase the surface area of the catalyst (from 4.9 to 28.02 m^2/g) and provide enough chance for the substrates to access to the catalytic active sites.

Fig. 4

Shown in Fig. 4, great changes of TEM image of the catalyst **4d** have taken place according to ZnPS-PVPA. TEM photography of ZnPS-PVPA (Fig. 4A) manifests the spheroid structure and the sizes of the particle in the range of 70-80 nm. While for the catalyst **4d** (Fig. 4B), the configuration is loose. The channels, holes and cavums could be also discerned clearly. Therefore, the catalysts could provide enough space for the epoxidation of unfunctionalized olefins and the substrates would approach the internal catalytic active sites easily in the solution.

Table 2

On behalf of exploring the control of chirality of products, ZnPS-PVPA and **3d** as well as homogeneous catalyst **6** are employed to epoxidize indene with m-CPBA/NMO. Low olefin enantio excesses are obtained (ee, 0% in entry 7 and 16.83% in entry 8, repectively), which confirms that both ZnPS-PVPA and **3d** are stereochemically inactive for the epoxidation of olefins. Then, ee values increase from 54% to 86.7% (Jacobsen's vs **6**, entry 1 vs entry 9) through the modification of alkyldiamine and further increase to 98% (**6** vs **4d**, entry 9 vs entry 5) upon immobilizing on ZnPS-PVPA. In view of these results, it could be deduced that the whole supported chiral salen Mn (Ⅲ) catalysts include the support ZnPS-PVPA, the linkage alkyldiamine as well as chiral salen Mn center together contribute to the chirality of products. Apart from this, ee values increase from 81% to 98%, conversions from 80% to >99% (entry 2-5) with the increase of carbon number of alkylamine in the asymmetric epoxidation of indene, which have been reported by C. Li [30] and our group [21]. Moreover, the catalytic activities of the catalyst 4d (conv%, >99 vs 51; ee, 98 vs 8; entry 5 vs 10) and the homogeneous catalyst 6 (conv%, 89 vs 76; ee, 86.7 vs 82.5; entry 9 vs 10) obviously increase with the addition of NMO in the epoxidation of indene, which is in accordance with the most articles reported [19-21].

According to NaClO/PPNO, the catalysts **4a-d** manifest higher catalytic abilities than Jacobsen's catalyst (conv%, 85 - >99 vs >99; ee%, 88 - >99 vs 65; entry 12-15 vs entry 11) and homogeneous catalyst **6** (conv%, 85 - >99 vs 86.2; ee%, 78 - >99 vs 92.6; entry 12-15 vs entry 17). Notably, homogeneous catalyst **6** indicates 92.6% ee upon the modification of Jacobsen's catalyst (ee, 65%) and the catalytic ability keeps on increasing (ee, up to >99%) after the catalyst **6** is immobilized on ZnPS-PVPA. Meanwhile, the catalytic activity indicates similar varying tendency to m-CPBA/NMO, accompanying with the increase of the chain length in the epoxidations of α-methylstyrene (conv%, from 85 to >99; ee, from 88 to >99; entry 12-15). In addition, ee values still increase in the presence of PPNO (ee%: 81 vs >99, entry 16 vs 15; 67.5 vs 92.6, entry 18 vs 17), which agrees with the most literatures reported [19-21].

As for $NaIO_4$/imidazole, the heterogeneous catalysts **4a-d** display superior catalytic properties to Jacobsen's catalyst (ee%, >99 vs 69; entry 20-23 vs entry 19) and comparable catalytic abilities to the catalyst **6** (conv%, >99 vs 86; ee%, >99 vs 82; entry 20-23 vs 25). Simultaneously, ee values vary from 69% (Jacobsen's catalyst, entry 19) to 82% (the catalyst 6**,** entry 25**)** through the modification of alkyldiamine, followed by going on increasing to >99% (the catalyst 4d, entry 23) upon the immobilization of the catalyst **6** onto ZnPS-PVPA. Moreover, both the conversions and enantioselectivities of the catalysts **4a-d** all exceed 99%, which is not involved in the length of the linkage. Interestingly, the superior catalytic activities could still be maintained whether the axial ligand imidazole is added or not (conv%, >99 vs >99; ee%, >99 vs >99; entry 23 vs entry 24). While for the homogeneous catalyst **6,** the catalytic disposition increase a little in the presence of imidazole (conv%, 86 vs 83; ee%, 82 vs 79, entry 25 vs 26). In view of the results reported, the catalytic tests indicate excellent catalytic abilities (conv%, 97; ee%, >99) in the absence of axial ligand imidazole and lower abilities (conv%, 70; ee%, 88) [31] with the addition of imidazole.

Table 3

After recycling for twelve consecutive times, the results are listed in Table 3. Notably, the catalytic ability decreases slightly and still indicates favourable disposition in the ninth recycling (conv.%, 89; ee%, 91). The effective separating the chiral salen Mn(III) complexes by the solid support ZnPS-PVPA could avoid the generation of the inactive μ-oxo-Mn(IV) species and ultimately could contribute to the superior stability of the catalyst. The decrease of the yield could be attributed to the decomposition of the chiral Mn (III) salen complex under epoxidative conditions[32] and the loss of the hyperfine granules of the heterogeneous chiral Mn (III) salen catalysts. The Mn content of the catalyst **4d** reduces from 0.73 mmol/g (the fresh) to 0.45 mmol/g after recycling for 9 times.

In summary, chiral salen Mn(III) anchored onto ZnPS-PVPA upon alkyldiamines have been synthesized and indicate comparable or even higher enantioselectivities than homogeneous catalyst. Moreover, the supported chiral Mn (III) salen catalysts are relatively stable and could be recycled nine times in the asymmetric epoxidation of α-methylstyrene. Our present investigation points to the generation of a general platform that will pave the way for heterogeneous epoxidation reactions of alkenes generating no Mn catalyst waste and allowing continuous recycling.

Supplementary data

FT-IR spectra, UV-vis spectrum, Experimental section.

Acknowledgement

This work is financially supported by the Fundamental Research Funds for the Central Universities (XDJK2013C120), the Xihua University Key Projects (Z1223321), Sichuan Province Applied Basic Research Projects (2013JY0090), the Department of Education of Sichuan Province Projects (13ZB0030), Chongqing Special Funding for Postdoctoral (Xm2014028) and Chongqing Postdoctoral Daily Fund (Rc201419).

References

[1] E. N. Jacobsen, W. Zhang, M. L. Guler, J. Am. Chem. Soc, 113 (1991) 6703-6704.

[2] V. L. P. Fragola, F. Lupo, A. Pappalardo, G. T. Sfrazzetto, R. M. Toscano, F. P. Ballistreri, G. A. Tomasellia, A. Gulino, J. Mater. Chem , 22 (2012) 20561-20565.

[3] A. F. Trindade, P. M. P. Gois, C. A. M. Afonso, Chem. Rev, 109 (2009) 418-514.

[4] T. P. Yoon, E. N. Jacobsen, Science, 299 (2003) 1691-1693.

[5] I. W. E. E. Arends, Angew. Chem. Int. Ed, 45 (2006) 6250-6252.

[6] D. Y. Xie, S. B. Sharma, N. L. Paiva, D. Ferreira, R. A. Dixon, Science, 299 (2003) 396-399.

[7] Q. H. Xia, H. Q. Ge, C. P. Ye, Z. M. Liu, K. X. Su, Chem. Rev, 105 (2005) 1603-1662.

[8] M. L. Merlau, M. D. P. Mejia, S. T. Nguyen, J. T. Hupp, Angew. Chem. Int. Ed, 22 (2001) 4369-4372.

[9] Corma A and Garcia H (2008) Supported gold nanoparticles as catalysts for organic reactions, Chem Soc Rev, 37: 2096-2126.

[10] B. M. Rossbach, K. Leopold, R. Weberskirch, Angew. Chem. Int. Ed, 45 (2006) 1309-1312.

[11] C. Baleizão, H. Garcia, Chem. Rev, 106 (2006) 3987-4043.

[12] A. Zulauf, M. Mellah, X. Hong, E. Schulz, Dalton Trans, 39 (2010) 6911-6935.

[13] J. M. Thomas, R. Raja, Acc Chem Res, 41 (2008) 708-720.

[14] S. Bell, B. Wustenberg, S. Kaiser, F. Menges, T. Netscher, A. Pfaltz, Science, 311 (2006) 642-644.

[15] M. Wills, Science, 311 (2006) 619-620.

[16] R. Raja, J. M. Thomas, M. D. Jones, B. F. G. Johnson, D. E. W. Vaughan, J. Am. Chem. Soc, 125 (2003) 14982-14983.

[17] C. Bianchini, P. Barbaro, 19 (2002) 17-32.

[18] J. M. Fraile, J. I. García, C. I. Herrerías, J. A. Mayoral, E. Pires, Chem Soc Rev, 38 (2009) 695-706.

[19] W. S. Ren, X. K. Fu, H. B. Bao, R. F. Bai, P. P. Ding, B. L. Sui, Catal Commun, 10 (2009) 788-793.

[20] X. B. Tu, X. K. Fu, X. Y. Hu, Hu, Y. D. Li, Inorg Chem Commun, 13 (2010) 404-407.

[21] B. W. Gong, X. K. Fu, J. X. Chen, Y. D. Li, X. C. Zou, X. B. Tu, P. P. Ding, L. P. Ma, J Catal , 262 (2009) 9-17.

[22] J. Huang, X. K. Fu, G. Wang, C. Li, X. Y. Hu, Dalton Trans, 40 (2011) 3631-3639.

[23] J. Huang, X. K. Fu, G. Wang, Q. Miao, Dalton Trans , 41 (2012) 10661-10669.

[24] J. Huang, X. K. Fu, Q. Miao, Appl Catal A, 407 (2011) 163-172.

[25] J. Huang, X. K. Fu, Q. Miao, Catal Sci Technol, 1 (2011) 1472-1482.

[26] J. Huang, M. Tang, X. Li, G. Z. Zhong, C. M. Li, Dalton Trans, 43 (2014) 17500-17508.

[27] H. D. Zhang, Y. M. Zhang, C. Li, J Catal, 238 (2006) 369-381.

[28] X. Y. Hu, X. K. Fu, J. W. Xu, C. W. Wang, J Organomet Chem, 696 (2011) 2797-2804.

[29] C. E. Song, E. J. Roh, B. M. Yu, D. Y. Chi, S. C. Kim, K. J. Lee, Chem Commun, **7** (2000) 615-616.

Figures captions:

Scheme 1 Synthesis of the heterogeneous catalysts

Scheme 2 Synthesis of homogeneous catalysts

Fig 1 TG curves of heterogenerous catalyst 4d

Fig 2 The nitrogen adsorption-desorption isotherm and pore distribution of the catalyst 4d

Fig 3 SEM photograph of (A) ZnPS-PVPA and (B) the catalyst 4d

Fig 4 TEM photograph of (A) ZnPS-PVPA and (B) the catalyst 4d

Fig. S1 FT-IR spectra of (1) 4d; (2) the neat chiral salen Mn (III)

Fig. S2 Solid reflectance UV-vis spectra (A) the neat chiral salen Mn (III);(B)the catalyst 4d

Tables

Table 1 The physical properties of ZnPS-PVPA, 2 and 4d

Sample	Surface area (m^2/g)	Pore volum ($\times 10^{-2}$ cm^3/g)	Average pore diameter (nm)	Mn content (mmol/g)
1	4.9	1.3	3.5	-
2	36.9	18.82	10.21	-
4d	28.02	4.442	0.61	0.73

Table 2 Asymmetric epoxidation of α-methylstyrene and indene catalyzed by homogeneous and heterogeneous catalysts (4a-h) with m-CPBA/NMO[a], NaClO/PPNO[b] and $NaIO_4$/imidazole[c] as oxidant systems

Entry	Substrate[d]	Catalyst	Oxidant system	Time	Conv.(%)	ee[e]	TOF[f]$\times 10^{-4}$(s^{-1})
1	A	Jacobsen’s	m-CPBA/NMO	1	98	54	54.42
2	A	4a	m-CPBA/NMO	1	80	81	44.44
3	A	4b	m-CPBA/NMO	1	82	85	45.58
4	A	4c	m-CPBA/NMO	1	92	92	51.09
5	A	4d	m-CPBA/NMO	1	>99	98	54.99
6	A	4d	m-CPBA	1	51	8	28.35
7	A	ZnPS-PVPA	m-CPBA/NMO	1	>99	0	54.99
8	A	3d	m-CPBA/NMO	1	>99	16.83	54.99
9	A	6	m-CPBA/NMO	1	89	86.7	49.44
10	A	6	m-CPBA	1	76	82.5	42.21
11	B	Jacobsen’s	NaClO/PPNO	24	>99	65	2.31
12	B	4a	NaClO/PPNO	24	85	88	1.96
13	B	4b	NaClO/PPNO	24	87	90	2.02
14	B	4c	NaClO/PPNO	24	94	91	2.18
15	B	4d	NaClO/PPNO	24	>99	>99	2.29
16	B	4d	NaClO	24	65	81	1.30
17	B	6	NaClO/PPNO	24	86.2	92.6	1.99
18	B	6	NaClO	24	82	67.5	1.90
19	B	Jacobsen’s	$NaIO_4$/imidazole	5	>99	69	11.11
20	B	4a	$NaIO_4$/imidazole	5	>99	>99	11.11
21	B	4b	$NaIO_4$/imidazole	5	>99	>99	11.11
22	B	4c	$NaIO_4$/imidazole	5	>99	>99	11.11
23	B	4d	$NaIO_4$/imidazole	5	>99	>99	11.11
24	B	4d	$NaIO_4$	5	>99	>99	11.11
25	B	6	$NaIO_4$/imidazole	5	86	82	9.65
26	B	6	$NaIO_4$	5	83	79	9.31

[a] Reactions were carried out at -20 °C in CH_2Cl_2 (3 mL) with indene (1 mmol), n-nonane (internal standard, 1 mmol), NMO (5 mmol), homogeneous (5 mol%) or heterogeneous salen Mn(III) catalysts (5 mol%) and m-CPBA (2 mmol). The conversion and the ee value were determined by GC with chiral capillary columns HP19 091G-B213, 30 m × 0.32mm × 0.25 μm.

[b] Reactions were carried out at 20 ℃ in CH_2Cl_2 (2 mL) with α-methylstyrene (1 mmol), PPNO (0.38 mmol) and NaClO (pH 11.5, 0.55 M, 3 mL). Other conditions are the same as aforementioned.

[c] Reactions conditions: alkene (1 mmol), $NaIO_4$ (2 mmol), catalyst (0.03mmol), CH_3CN/H_2O (10 mL/5 mL).

[d] A = indene, B = α-methylstyrene.

[e] (S)-form.

[f] Turnover frequency (TOF) is calculated by the expression of [product]/[catalyst] × time (s^{-1}).

Table 3 The recycles of catalyst **4d** in the asymmetric epoxidation of *α*-methylstyrene[a]

Run	Time	Conversion (%)	*ee*[b] (%)	TOF[c]$\times 10^{-4}$(s^{-1})
1	24	>99	>99	2.31
2	24	99	99	2.29
3	24	98	98.5	2.27
4	24	97	98.1	2.25
5	24	95	96.6	2.20
6	24	93	96	2.15
7	24	91	95.4	2.11
8	24	90	92	2.09
9	24	89	91	2.06
10	24	84	87.6	1.94
11	24	82	82.1	1.90
12	24	75	76	1.74
13	24	67	62	1.55

[a] Reactions were carried out at -40 ℃ in CH_2Cl_2 (4 mL) with *α*-methylstyrene (1 mmol), *n*-nonane (internal standard, 1 mmol), m-CPBA (0.38 mmol), heterogeneous salen Mn (III) catalysts (5 mol%). The conversion and the ee value were determined by GC with chiral capillary columns HP19091G-B213, 30 m×0.32 mm×0.25 μm.

[b] Same as in Table 2.

[c] Same as in Table 2.

Figures

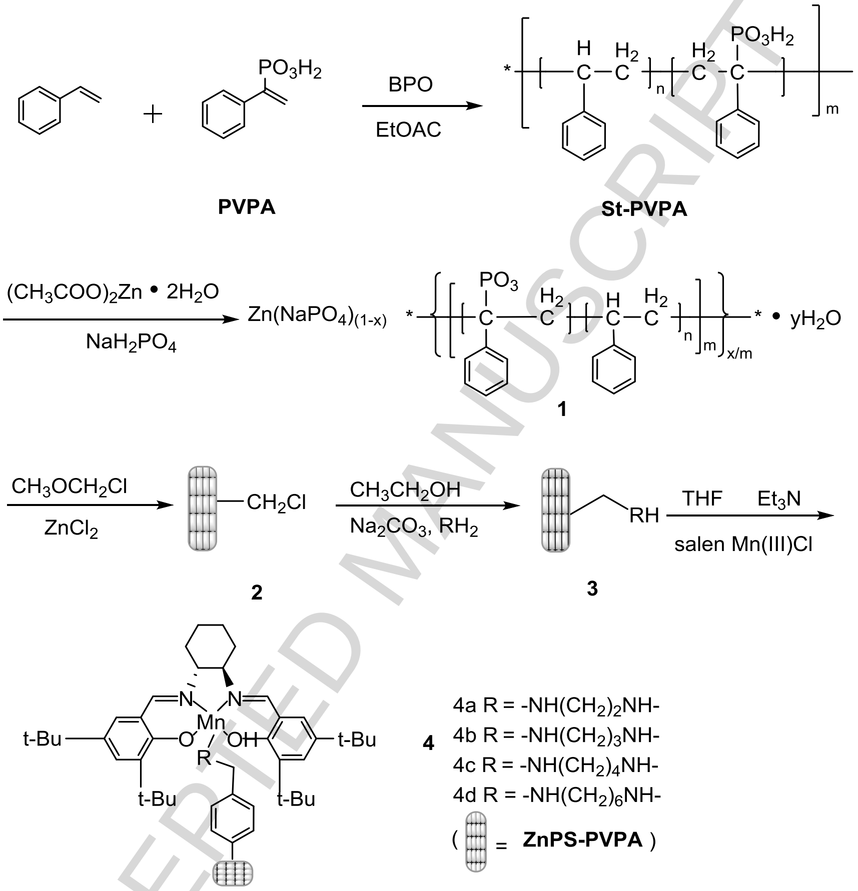

Scheme 1

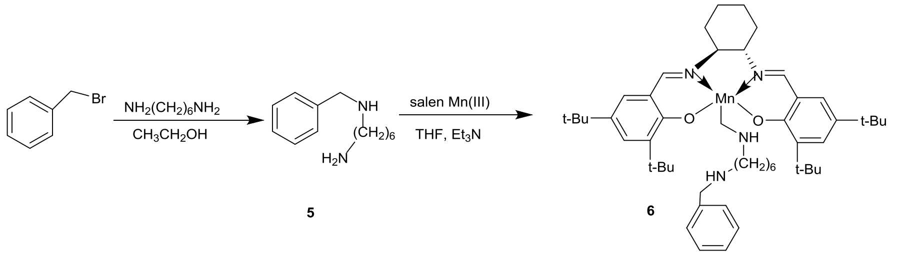

Scheme 2

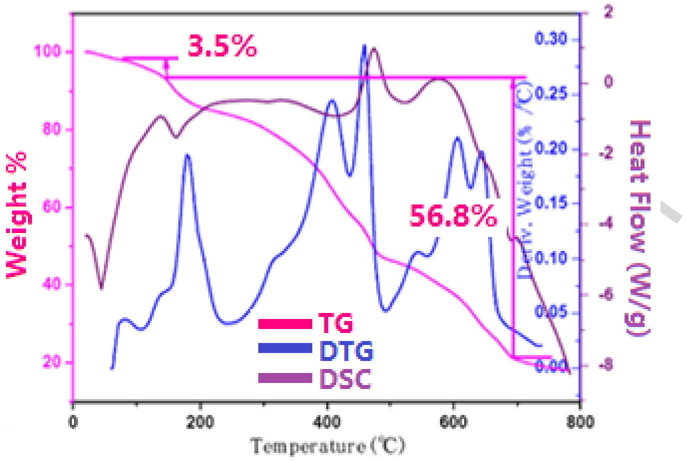
3.5%
56.8%
Weight %
100
80
60
40
20
0
200
400
600
800
Temperature (℃)
Deriv. Weight (% /℃)
0.30
0.25
0.20
0.15
0.10
0.05
0.00
Heat Flow (W/g)
2
0
-2
-4
-6
-8
TG
DTG
DSC

Fig 1

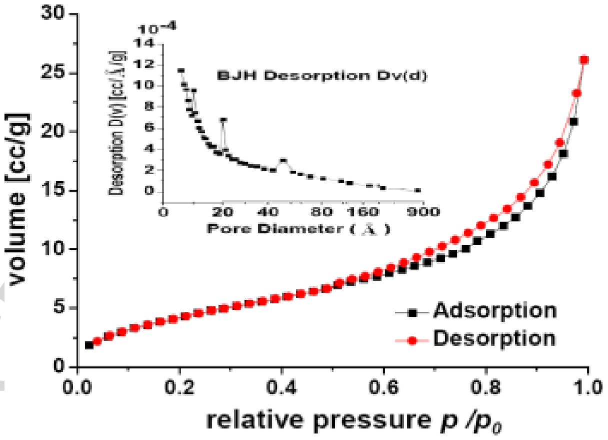
volume [cc/g]
30
25
20
15
10
5
0
0.0
0.2
0.4
0.6
0.8
1.0
relative pressure p /p0
Adsorption
Desorption
BJH Desorption Dv(d)
10^-4
Desorption D(v) [cc/Å/g]
14
12
10
8
6
4
2
0
20
40
80
160
900
Pore Diameter (Å)

Fig 2

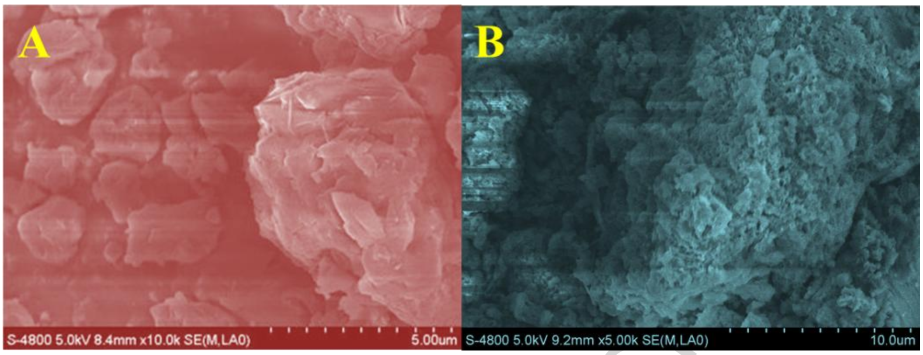
A
B
S-4800 5.0kV 8.4mm x10.0k SE(M,LA0)
5.00um
S-4800 5.0kV 9.2mm x5.00k SE(M,LA0)
10.0um

Fig 3

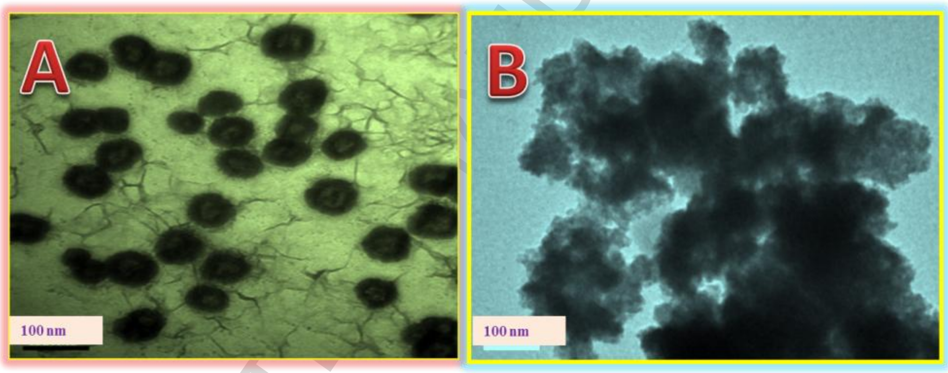
A
B
100 nm
100 nm

Fig 4

Graphic Abstract-pictogram

Layered crystalline chiral salen Mn(III) complexes immobilized on organic polymer–inorganic hybrid zinc phosphonate-phosphate as efficient and reusable catalysts for the unfunctionalized olefin epoxidation

Jing Huang,*[a,b] Jiali Cai,[c] Chenxiao Hong[a]

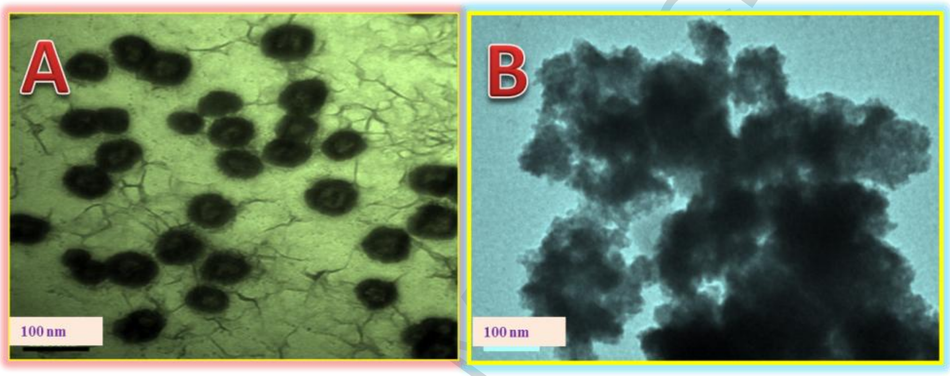

Graphical abstract-synopsis

The catalysts that alkyldiamines modified ZnPS-PVPA are used for the immobilization of chiral salen Mn (III) display superior catalytic ability either for the experimental scale reactions or for the large-scale reactions.

Highlights

- The chiral salen Mn(III) is immobilized on alkyldiamines modified ZnPS-PVPA
- The heterogeneous catalysts display superior activity according to the homogeneous catalysts
- The heterogeneous catalysts could be reused at least nine times without significant loss of activity
- The catalysts could be used in large-scale reactions with superior catalytic disposition